

## Research Article

**Cite this article:** Hays BR, Riginos C, Palmer TM, Gituku BC, and Goheen JR (2020) Using photography to estimate above-ground biomass of small trees. *Journal of Tropical Ecology* 36, 213–219. <https://doi.org/10.1017/S0266467420000139>

Received: 1 October 2019  
Revised: 30 April 2020  
Accepted: 3 June 2020  
First published online: 23 September 2020

**Keywords:**

*Acacia*; herbivory; photographic analysis; remote sensing; savanna

**Author for correspondence:**

\*Brandon R. Hays, Email: [bhays3@uwyo.edu](mailto:bhays3@uwyo.edu)

Brandon R. Hays<sup>1,\*</sup>, Corinna Riginos<sup>2</sup>, Todd M. Palmer<sup>3</sup>, Benard C. Gituku<sup>4,5</sup> and Jacob R. Goheen<sup>1</sup>

<sup>1</sup>Department of Zoology and Physiology, University of Wyoming, Laramie, WY 82071, USA; <sup>2</sup>The Nature Conservancy, 258 Main Street, Lander, WY 82520, USA; <sup>3</sup>Department of Biology, University of Florida, Gainesville, 32611 Florida, USA; <sup>4</sup>Department of Land Resource Management & Agricultural Technology, University of Nairobi, P.O. Box 30197, Nairobi, Kenya and <sup>5</sup>Ol Pejeta Conservancy, 10400 Nanyuki, Kenya

**Abstract**

Quantifying tree biomass is an important research and management goal across many disciplines. For species that exhibit predictable relationships between structural metrics (e.g. diameter, height, crown breadth) and total weight, allometric calculations produce accurate estimates of above-ground biomass. However, such methods may be insufficient where inter-individual variation is large relative to individual biomass and is itself of interest (for example, variation due to herbivory). In an East African savanna bushland, we analysed photographs of small (<5 m) trees from perpendicular angles and fixed distances to estimate above-ground biomass. Pixel area of trees in photos and diameter were more strongly related to measured, above-ground biomass of destructively sampled trees than biomass estimated using a published allometric relation based on diameter alone ( $R^2 = 0.86$  versus  $R^2 = 0.68$ ). When tested on trees in herbivore-exclusion plots versus unfenced (open) plots, our predictive equation based on photos confirmed higher above-ground biomass in the exclusion plots than in unfenced (open) plots ( $P < 0.001$ ), in contrast to no significant difference based on the allometric equation ( $P = 0.43$ ). As such, our new technique based on photographs offers an accurate and cost-effective complement to existing methods for tree biomass estimation at small scales with potential application across a wide variety of settings.

**Introduction**

Allometric relationships enable the estimation of above-ground biomass of trees from structural measurements (e.g. diameter, height, crown breadth; Chave *et al.* 2005, Henry *et al.* 2011, Pastor *et al.* 1984, Young *et al.* 1964). This approach is most useful for individuals of large size which exhibit little variation in structure relative to overall biomass (e.g. rainforest trees). However, in populations with greater structural heterogeneity relative to total biomass, allometric relationships may be unreliable (Antonio *et al.* 2007, Dutcă *et al.* 2017). Such variation among individuals can arise from a number of factors, including structural modification of trees due to herbivory (Whitham & Mopper 1985), parasitism (Stanton *et al.* 1999), competition (Poorter *et al.* 2012) or abiotic conditions (Copenhaver & Tinker 2014). Therefore, in systems where structural heterogeneity is both large relative to individual biomass and itself of interest to researchers, methods that accurately quantify such variation are needed.

Recent advances in remote sensing technologies have made it possible to rapidly quantify such individual variation. LiDAR (Light Detection And Ranging) can generate highly accurate (<1 cm spacing) point clouds from which 3D models of trees can be constructed (Raumonen *et al.* 2015, Yao *et al.* 2012) and their biomass estimated (Gonzalez de Tanago *et al.* 2018, Popescu 2007). However, LiDAR is prohibitively expensive for many, with a standard sensor costing \$115 000 from the manufacturer (Rieglusa.com). Commissioning airborne LiDAR surveys may be cheaper but still costs tens of thousands of dollars. These techniques may be cost-effective if large tracts of land need to be surveyed, however for smaller scale studies they are unsuitable. In an attempt to balance affordability, simplicity and accuracy, we developed a technique to estimate above-ground biomass via photography and freely available image analysis software.

We sought to reliably assess above-ground biomass of *Acacia* (*Vachellia*) *drepanolobium*, a small (<5 m tall) savanna tree that forms monodominant stands across large tracts (100–1000s of km<sup>2</sup>) in central Kenya (Young *et al.* 1997b). As both a nitrogen fixer (Fox-Dobbs *et al.* 2010) and a key component of several large mammals' diets (Birkett 2002, Kartzinel *et al.* 2015), *A. drepanolobium* is an important driver of ecosystem function. It is also a myrmecophyte (ant plant) which may host any of four intensely competing ant species offering varying degrees of protection against herbivores in exchange for food (extra-floral nectar) and shelter (modified stipular spines) (Palmer *et al.* 2008, 2010). Because the various species of ant occupants differentially



**Figure 1.** Two photographs of the same tree in 2017 (left) and 2019 (right) showing the extent of elephant damage on canopy.

modify the architecture of *A. drepanolobium*, trees of the same trunk diameter can have drastically different canopy shapes (Stanton *et al.* 1999). In addition, elephants can dramatically alter tree canopy by ripping off large segments during feeding, removing anywhere from 10–100% of branches (Figure 1). As a result, variation amongst *A. drepanolobium* can be as large as the total biomass of individual trees. For example, two trees of equal diameter may differ in biomass by orders of magnitude when one tree has had its entire canopy removed via elephant herbivory. We developed our photographic technique to quantify this variation due to herbivory and ant occupant. Accordingly, we trained our method on trees with multiple species of ant occupant and validated the method in replicated unfenced and herbivore-exclusion plots.

## Methods

### Study site

We worked at Mpala Research Centre (0°17'54.0"N, 36°52'16.4"E) and Ol Pejeta Conservancy (0°02'01.7"N, 36°52'59.9"E) in Laikipia County, Kenya. Here, as in many other parts of East Africa underlain by black cotton soils, *A. drepanolobium* forms the vast majority (~98%) of tree cover (Goheen & Palmer 2010, Pringle *et al.* 2016, Young *et al.* 1997a). Throughout most of its range, *A. drepanolobium* exhibits variable canopy volume and a maximum height of 3–5 m (Okello *et al.* 2001); trees >3 m are rare at our study sites.

### Tree selection

We selected a sample of 30 *A. drepanolobium* trees at Mpala Research Centre, ranging from 0.5–2.5 m tall and with diameters from 3–10 cm. We measured height and diameter; we measured diameter at 30 cm above the ground and marked the position with red paint. To account for variation in tree architecture, we selected trees that were occupied by the most common species of ant symbionts (Stanton *et al.* 1999). We selected 10 trees occupied by the less common *Crematogaster nigriceps*, which tend to exhibit smaller, more condensed architectures, and 20 trees occupied by the more common *C. mimosae*, which reach a greater height but have sparser canopies.

### Photo acquisition

Using a 4-megapixel Nikon Coolpix 4500 mounted on a 1 m tripod, we took two photos of each tree at perpendicular angles to account for anisotropy. For each photo, the camera was placed 4 m from the tree and aligned either due north or east as measured by a high accuracy GPS compass (Garmin GPSMAP 64st). In cases where obstacles prevented camera placement due north or due east, both photo points were offset equally to maintain perpendicular orientations. We then used a bubble level to adjust the tripod until the camera was level relative to the ground. We also included a ruler at a fixed position for scale. The ruler was placed equidistant between the two photo points, 3.5 m from each point and 0.5 m from the tree. Once the camera and ruler were situated, a large, red-fabric sheet was erected behind the tree to maximize contrast (Figure 2). The photograph was taken at minimum zoom (38 mm focal length in 35 mm camera equivalent) and at maximum resolution (2272 × 1704 pixels) in manual mode, so that aperture and shutter speed could be manipulated for maximum contrast between tree and sheet. We repeated this process for each tree for a total of 60 photos (2 photos per tree for 30 trees).

### Destructive sampling

After the trees had been photographed, they were cut down and all components above the diameter measurement were collected in large bags for drying (Okello *et al.* 2001). To ensure that photo pixels and their associated areas corresponded to actual canopy size, for each tree we measured the sum of the lengths of all tree branches >2 cm in diameter (hereafter 'running branch length'). The tree components in bags were left out in the sun during the dry season and weighed every week until measurements stabilized; they were measured for another 2 weeks after this point to ensure constant dry weight had been reached. After 2 months, all trees had achieved a constant weight and final dry weight measurements were taken.

### Photo analysis

We attempted to isolate trees from background using automated and manual methods for photo analysis in three different software packages: ImageJ, ArcGIS and GIMP. In ImageJ, we



**Figure 2.** Photograph setup in the field, with camera situated 4 m from the target tree and oriented to 0°.

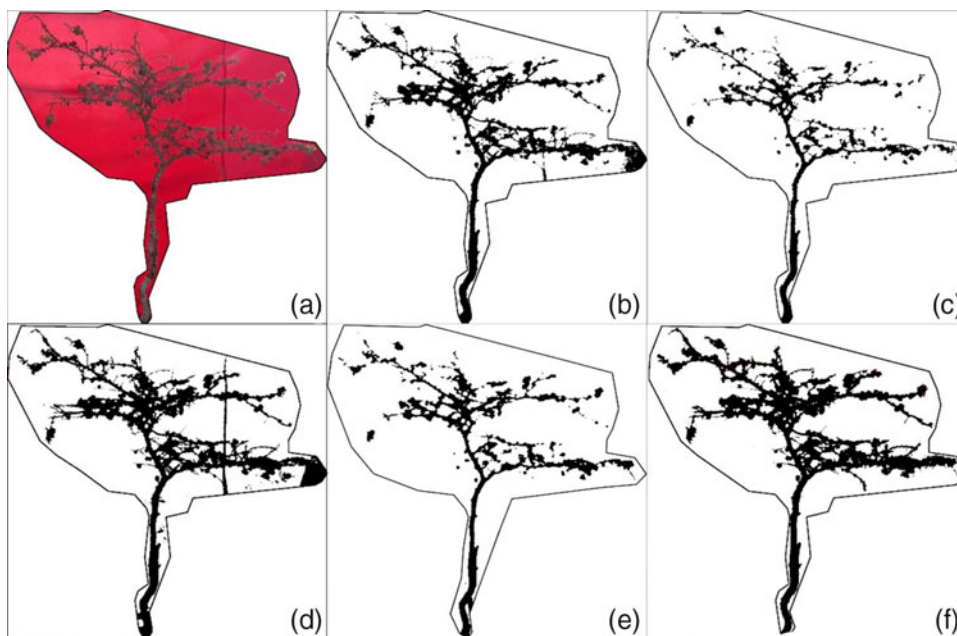


**Figure 3.** An individual *A. drepanolobium* photo-cropped (a), auto-thresholded using the three best algorithms in ImageJ (IsoData, Minimum and Otsu, b–d), classified using a supervised maximum likelihood classification in ArcGIS (e), and manually classified in GIMP (f).

used several auto-thresholding algorithms, which binarize an image into background and object pixels based on different mathematical approaches. In ArcGIS, we used both supervised and unsupervised maximum likelihood classifications. Comparing the resultant classifications visually, we found that analysing photos manually in GIMP (GNU Image Manipulation Program), a freely available image editing software, was the most accurate means of isolating trees from background (Figure 3).

We used the following procedure in GIMP. First, photos were cropped to include only the portion of the tree above the red-painted diameter mark. Then, we used the ‘select by color’ tool to select and delete all pixels with colour values similar to a sample

of pixels from the (red) background sheet. This process was iterated until only the tree pixels remained in the photo (hereafter ‘pixels’). The resolution of the original photo could be determined using the included ruler (cm<sup>2</sup>/pixel). The area of the tree was then calculated from this known scale and the total number of pixels remaining in the photo (hereafter ‘area’).

#### Data analysis

Using individual tree dry weight as our response variable, we created two competing multiple linear regression models. The predictors of the two models were a series of covariates plus either photo pixels or



area (since area was derived from photo pixels, they could not both be included in the same model; Equations 1 and 2).

$$\text{Biomass (kg)} \sim \text{Pixels} + \text{Diameter (cm)} + \text{Height (m)} \\ + \text{Running Branch Length (cm)} + \text{Ant Species} \quad \text{Eqn 1}$$

$$\text{Biomass (kg)} \sim \text{Area (cm}^2\text{)} + \text{Diameter (cm)} + \text{Height (m)} \\ + \text{Running Branch Length (cm)} + \text{Ant Species} \quad \text{Eqn 2}$$

The pixel values in perpendicular photos of the same tree were averaged to create the model variable; the same was done for area. The final candidate model was determined via backwards stepwise model selection by AIC using the stepAIC function from the MASS package in R (Venables & Ripley 2002). We evaluated the accuracy of the model by k-fold cross validation, splitting the 30 test trees into five groups and evaluating a model created from 80% of the data against the remaining 20%, repeated 1000 times (Kuhn 2019). The predictions of the final regression model were compared with an existing allometric equation for *A. drepanolobium* (Okello *et al.* 2001; Equation 3).

$$\text{Biomass (kg)} = e^{\ln(\text{diameter}) * 2.2949 + 4.7997} / 1000 \quad \text{Eqn 3}$$

We performed all statistical analyses using R statistical software (R Core Team 2018); regressions were carried out using the lm() function and relative importance of variables was assessed with the 'relaimpo' package (Grömping 2006).

### Model validation

Finally, we used the regression to predict biomass for selected trees within twelve 0.5-ha herbivore-exclusion plots of a separate experiment started in 2017 at Ol Pejeta Conservancy. Half of the plots were fenced to keep out elephants and other large (>30 kg) ungulates, and half were left unfenced. Paired fenced and unfenced plots are separated by less than 50 m to control for effects of precipitation and soil, and all plots were located in the same 37.5 km<sup>2</sup> area. A stratified random sample of tagged trees within these plots have been measured annually for a separate demographic study. We used a subset of these trees to validate our model: those that could be physically photographed (i.e. were not obstructed by other closely growing trees) and were in the same 0.5–2.5 m height range as the trees used in model training. We photographed 10 trees in each plot (for a total of 120 trees). On a windless day, it took ~1.5 hours to photograph 10 trees; therefore, to photograph all trees within a 0.5 ha plot (60–70) under ideal conditions would take ~12 hours. The plots had been fenced for 2 years by the time of photographing and showed significant differences in tree measurements (Table 1); we therefore expected differences in tree biomass between the unfenced and fenced areas. Finally, we applied Okello *et al.*'s regression to the same trees for comparison.

### Results

Running branch length was positively correlated with tree area calculated from photographs ( $r = 0.90$ ) and significantly related to model predicted biomass ( $R^2 = 0.83$ ,  $P < 0.001$ ), demonstrating that photo-derived area accurately represents tree canopy area.

The final (best) regression model for tree biomass included only diameter and tree area in photos, with  $R^2 = 0.86$  after cross validation

**Table 1.** Means and standard errors about means for tree measurements in the experimental plots used for model validation, with 380 trees in fenced plots and 385 trees in open plots

|                               | Fenced  |        | Open    |        | 2-sided t-test |
|-------------------------------|---------|--------|---------|--------|----------------|
|                               | Mean    | SEM    | Mean    | SEM    |                |
| Height (m)                    | 1.83    | 0.06   | 1.30    | 0.06   | $P < 0.001$    |
| Diameter (cm)                 | 5.00    | 0.17   | 4.38    | 0.20   | $P = 0.02$     |
| Basal area (cm <sup>2</sup> ) | 28.57   | 1.77   | 27.42   | 2.25   | $P = 0.69$     |
| Pixel area (cm <sup>2</sup> ) | 8714.97 | 630.40 | 3342.64 | 472.08 | $P < 0.001$    |

**Table 2.** Parameters for the final regression, with  $R^2 = 0.86$

|           | Parameter estimate | Standard error | Probability | Variation explained |
|-----------|--------------------|----------------|-------------|---------------------|
| Intercept | -3.240             | 1.072          | <0.01       |                     |
| Area      | 0.0005259          | 0.00009901     | <0.01       | 46%                 |
| Diameter  | 0.9941             | 0.2343         | <0.01       | 40%                 |

(Table 2). Ant occupant was not a significant variable in the model, nor was there a significant difference in biomass based on ant species (2-sided t-test,  $P = 0.43$ ). Area was a slightly better predictor of biomass ( $R^2 = 0.86$  vs  $R^2 = 0.85$ ) and was used instead of pixels, since they were highly collinear. Height was highly correlated with diameter ( $r = 0.77$ ) and only accounted for a small amount of variation not accounted for by diameter ( $R^2 = 0.0056$ ).

The allometric equation of Okello *et al.* explained less variation ( $R^2 = 0.68$ ,  $RMSE = 2.97$ ) than our regression ( $R^2 = 0.86$ ,  $RMSE = 1.36$ , Figure 4). Squared residuals of the allometric predictions were significantly greater than our regression predictions (1-sided t-test,  $P = 0.02$ ).

Finally, average individual tree biomass within herbivore-exclusion plots, as modelled by our photographic regression, was significantly greater (1-sided t-test,  $P < 0.001$ ) in fenced plots (mean =  $7.75 \text{ kg} \pm 0.50 \text{ SEM}$ ) than in open plots (mean =  $4.52 \text{ kg} \pm 0.51 \text{ SEM}$ ). However, biomass modelled by the Okello *et al.* equation for the same subset of trees did not show a significant difference (1-sided t-test,  $P = 0.43$ ) between fenced plots (mean =  $9.44 \pm 0.70 \text{ SEM}$ ) and open plots ( $9.20 \pm 1.33 \text{ SEM}$ , Figure 5). Nor did the allometric equation show a significant difference in biomass when applied to all trees within plots (1-sided t-test,  $P = 0.48$ ).

### Discussion

Our photographic technique accurately predicted above-ground biomass of *A. drepanolobium* and was a substantial improvement over an existing allometric equation. Using this method, we were able to quantify the significant difference in above-ground biomass between unfenced and herbivore-exclosure plots, attributable to herbivore browsing. This contrast was apparent from a visual survey of the plots and was reflected in significant differences in tree height and diameter. However, the biomass estimates from the existing allometric equation of Okello *et al.* (2001) did not accurately capture these differences, demonstrating the need for a complementary method to quantify changes in biomass due to herbivory. In addition, we did not find an effect of ant occupant, suggesting that differences in architecture induced by ants do not

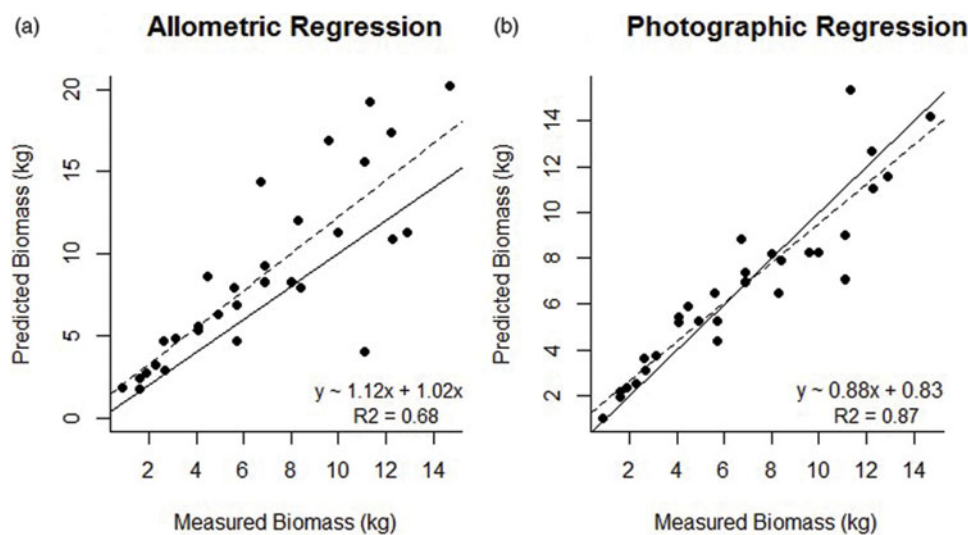


**Figure 4.** Plots showing measured tree biomass on the x-axis and model predicted biomass on the y-axis. The solid line represents a perfect 1-1 model and the dashed line represent simple linear regressions ( $n = 30$  trees) between measured weights and weights predicted by the (a) Okello *et al.* allometric equation and (b) the photographic regression of the current study. Linear regression equations and  $R^2$  values are included. The photographic regression ( $R^2 = 0.86$ ) performed better than the allometric equation ( $R^2 = 0.68$ ). Note that the linear regression of the allometric equation (A) falls wholly below the 1-1 line.

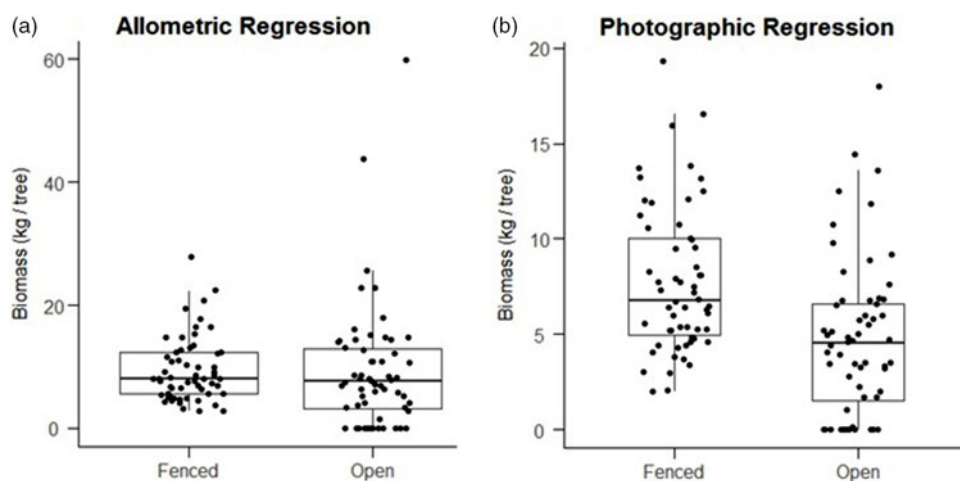


**Figure 5.** Boxplots showing the distribution of modeled biomasses for individual trees, pooled by fenced plots ( $n = 58$  trees) and open plots ( $n = 59$  trees). Predictions of the Okello allometric equation (a) do not show a significant difference between fenced and open plots (1-sided t-test,  $P = 0.43$ ). Predictions of the photographic regression (b) do show significantly greater biomass in fenced plots (1-sided t-test,  $P < 0.001$ ).

affect total biomass. Our photographic method provides an important extension to existing methods for quantifying changes in above-ground biomass.

In Laikipia and other regions of Kenya, *A. drepanolobium* is a key component of several large mammals' diets, including elephants (*Loxodonta africana*), reticulated giraffes (*Giraffa camelopardalis reticulata*) and black rhino (*Diceros bicornis*) (Birkett 2002, Kartzinel *et al.* 2015). Additionally, *A. drepanolobium* fixes nitrogen and partially drives nutrient dynamics and forage quality (Fox-Dobbs *et al.* 2010). Tracking changes in this acacia's biomass is therefore important for understanding both food availability for browsers and forage quality for all herbivores. This is particularly pertinent because *A. drepanolobium* in Laikipia County may experience wide-scale changes in abundance and cover due to increasing disturbance from invasive species (Riginos *et al.* 2015), charcoal harvesting (Okello *et al.* 2001) and land use change (Muriithi 2016).

Across most savannas, tree biomass and cover are important drivers of ecosystem structure and function (Holdo *et al.* 2009). Trees provide food for browsers, fix nutrients in soil, serve as habitat for arthropods and nesting sites for birds, and modify mammal movement and habitat use. Therefore, accurately measuring tree biomass is not only a desirable goal in itself but will also enhance our understanding of savanna ecology and aid in the management

of endangered species. Yet characterizing abundance, biomass and size structure of trees has been a long-standing challenge in savanna ecosystems (Archer 1996, House *et al.* 2003), particularly for remote sensing approaches (Munyati *et al.* 2011). While there have been photographic techniques developed to measure vegetative cover or shrub biomass (Louhaichi *et al.* 2010, 2017), these studies were conducted in arid regions in which low vegetation (forbs and shrubs) stood out starkly against a background of bare earth when viewed from above. In contrast, savannas are characterized by a matrix of grass that can be spectrally confused with the trees of interest (Cho *et al.* 2012). Likewise, a similar method (Ter-Mikaelian & Parker 2000) measured biomass on small, relatively isotropic seedlings that were not structurally altered by herbivory. But larger trees (1–3 m) present more 3-dimensional complexity and may suffer from significant asymmetry due to herbivory; consequently, they need to be photographed from multiple angles at ground level.

Our method is substantially less expensive than LiDAR, costing only a few hundred dollars for a camera, tripod and backdrop. It is ideal for small-scale projects in which it is inexpensive to employ 3–5 personnel to survey trees, although windy conditions can make holding the contrast backdrop physically taxing. However, our method is more laborious than LiDAR, and could not realistically

be used to measure trees at scales of tens or hundreds of hectares. In cases where larger scales are of interest, our technique will provide indispensable ground truth measurements by which to calibrate other forms of remote sensing, including LiDAR or aerial biomass estimates (Shepaschenko *et al.* 2019). In sum, our method provides an accurate, cost-effective and relatively efficient complement to existing methods for detecting changes in above-ground biomass of trees across space or through time.

A major obstacle is the extensive photo processing time required to classify photos of trees manually. If an accurate algorithmic classification scheme could be implemented, it would reduce the time investment considerably. Although our classification of photos was necessarily subjective, it was still considerably more accurate than any of the algorithmic approaches we attempted. Finally, those intending to use this technique should opt for the highest resolution (megapixel) camera available, as this will increase the accuracy of results.

Beyond savannas, accurately and efficiently estimating biomass of small trees should be useful for forest managers quantifying understorey biomass or comparing total biomass of a single species at different life stages (Hubau *et al.* 2019). In particular, it will be useful for measuring change in biomass of individual trees over time, allowing for more precise calculation of growth rates under different environmental conditions. A similar photographic technique was used to quantify tree architecture and measure similarity of traits between individuals in a study of herbivore community assembly (Barbour *et al.* 2015). Any study in which researchers wish to quantify browsing more accurately than commonly used qualitative metrics will also benefit from this method. We hope that this technique will find broad use with anyone seeking to measure above-ground biomass of relatively small (<5 m) trees.

**Acknowledgements.** We acknowledge the support of the National Science Foundation as well as the collaboration of Ol Pejeta Conservancy and Mpala Research Centre. J. Alston helped with coding, K. Driese reviewed this manuscript, and many helped with fieldwork: G. Busieni, S. Carpenter, J. Eckadeli, J. Gitonga, N. Maiyo, P. Milligan, G. Mizell, J. W. Murage, A. Njenga, A. Pietrek and K. Steinfield.

## References

- Antonio N, Tomé M, Tomé J, Soares P and Fontes L (2007) Effect of tree, stand, and site variables on the allometry of *Eucalyptus globulus* tree biomass. *Canadian Journal of Forest Research* **37**, 895–906.
- Archer S (1996) Assessing and interpreting grass–woody plant dynamics. In Hodgson J and Illius A (eds), *The Ecology and Management of Grazing Systems*. Wallingford: CAB International, pp. 101–134.
- Barbour MA, Rodriguez-Cabal MA, Wu ET, Julkunen-Tiitto R, Ritland CE, Miscampbell AE, Jules ES and Crutsinger GM (2015) Multiple plant traits shape the genetic basis of herbivore community assembly. *Functional Ecology* **29**, 995–1006.
- Birkett A (2002) The impact of giraffe, rhino and elephant on the habitat of a black rhino sanctuary in Kenya. *African Journal of Ecology* **40**, 276–282.
- Chave J, Andalo C, Brown S, Cairns MA, Chambers JQ, Eamus D, Fölster H, Fromard F, Higuchi N, Kira T and Lescure JP (2005) Tree allometry and improved estimation of carbon stocks and balance in tropical forests. *Oecologia* **145**, 87–99.
- Cho MA, Mathieu R, Asner GP, Naidoo L, van Aardt J and Ramoelo A (2012) Mapping tree species composition in South African savannas using an integrated airborne spectral and LiDAR system. *Remote Sensing of Environment* **125**, 214–226.
- Copenhagen PE and Tinker DB (2014) Stand density and age affect tree-level structural and functional characteristics of young, postfire lodgepole pine in Yellowstone National Park. *Forest Ecology and Management* **320**, 138–148.
- Putcã I, Mather R and Ioraş F (2017) Tree biomass allometry during the early growth of Norway spruce (*Picea abies*) varies between pure stands and mixtures with European beech (*Fagus sylvatica*). *Canadian Journal of Forest Research* **48**, 77–84.
- Fox-Dobbs K, Doak DF, Brody AK and Palmer TM (2010) Termites create spatial structure and govern ecosystem function by affecting N<sub>2</sub> fixation in an East African savanna. *Ecology* **91**, 1296–1307.
- Goheen JR and Palmer TM (2010) Defensive plant-ants stabilize megaherbivore-driven landscape change in an African savanna. *Current Biology* **20**, 1768–1772.
- Gonzalez de Tanago J, Lau A, Bartholomeus H, Herold M, Avitabile V, Raumonon P, Martius C, Goodman RC, Disney M, Manuri S, Burt A and Calders K (2018) Estimation of above-ground biomass of large tropical trees with terrestrial LiDAR. *Methods in Ecology and Evolution* **9**, 223–234.
- Grömping U (2006) Relative importance for linear regression in R: the package relaimpo. *Journal of Statistical Software* **17**, 1–27.
- Henry M, Picard N, Trotta C, Manlay R, Valentini R, Bernoux M and Saint André L (2011) Estimating tree biomass of sub-Saharan African forests: a review of available allometric equations. *Silva Fennica* **245**, 477–569.
- Holdo RM, Holt RD and Fryxell JM (2009) Grazers, browsers, and fire influence the extent and spatial pattern of tree cover in the Serengeti. *Ecological Applications* **19**, 95–109.
- House JI, Archer S, Breshears DD and Scholes RJ (2003) Conundrums in mixed woody–herbaceous plant systems. *Journal of Biogeography* **30**, 1763–1777.
- Hubau, W, De Mil T, Van den Bulcke J, Phillips OL, Ilondea BA, Van Acker J, Sullivan MJ, Nsenga L, Toirambe B, Couralet C and Banin LF (2019) The persistence of carbon in the African forest understorey. *Nature Plants* **5**, 133–140.
- Kartzinel TR, Chen PA, Coverdale TC, Erickson DL, Kress WJ, Kuzmina ML, Rubenstein DI, Wang W and Pringle RM (2015) DNA metabarcoding illuminates dietary niche partitioning by African large herbivores. *Proceedings of the National Academy of Sciences USA* **112**, 8019–8024.
- Kuhn M. Contributions from Wing J, Weston S, Williams A, Keefer C, Engelhardt A, Cooper T, Mayer Z, Kenkel B, the R Core Team, Benesty M, Lescarbeau R, Ziem A, Scrucca L, Tang Y, Candan C and Hunt T (2019) Classification and Regression Training. R package version 6.0-82. <https://CRAN.R-project.org/package=caret>.
- Louhaichi M, Johnson MD, Woertz AL, Jasra AW and Johnson DE (2010) Digital charting technique for monitoring rangeland vegetation cover at local scale. *International Journal of Agriculture and Biology* **12**, 406–410.
- Louhaichi M, Hassan S, Clifton K and Johnson DE (2017) A reliable and non-destructive method for estimating forage shrub cover and biomass in arid environments using digital vegetation charting technique. *Agroforestry Systems* **92**, 1341–1352.
- Munyati C, Shaker P and Phasha MG (2011) Using remotely sensed imagery to monitor savanna rangeland deterioration through woody plant proliferation: a case study from communal and biodiversity conservation rangeland sites in Mokopane, South Africa. *Environmental Monitoring and Assessment* **176**, 293–311.
- Muriithi FK (2016) Land use and land cover (LULC) changes in semi-arid sub-watersheds of Laikipia and Athi River basins, Kenya, as influenced by expanding intensive commercial horticulture. *Remote Sensing Applications: Society and Environment* **3**, 73–88.
- Okello BD, O'Connor, TG and Young TP (2001) Growth, biomass estimates, and charcoal production of *Acacia drepanolobium* in Laikipia, Kenya. *Forest Ecology and Management* **142**, 143–153.
- Palmer TM, Stanton ML, Young TP, Goheen JR, Pringle RM and Karban R (2008) Breakdown of an ant–plant mutualism follows the loss of large herbivores from an African savanna. *Science* **319**, 192–195.
- Palmer TM, Doak DF, Stanton ML, Bronstein JL, Kiers ET, Young TP, Goheen JR and Pringle RM (2010) Synergy of multiple partners, including freeloaders, increases host fitness in a multispecies mutualism. *Proceedings of the National Academy of Sciences USA* **107**, 17234–17239.
- Pastor J, Aber JD and Melillo JM (1984) Biomass prediction using generalized allometric regressions for some northeast tree species. *Forest Ecology and Management* **7**, 265–274.

- Poorter H, Niklas KJ, Reich PB, Oleksyn J, Poot P and Mommer L (2012) Biomass allocation to leaves, stems and roots: meta-analyses of interspecific variation and environmental control. *New Phytologist* **193**, 30–50.
- Popescu SC (2007) Estimating biomass of individual pine trees using airborne lidar. *Biomass and Bioenergy* **31**, 646–655.
- Pringle RM, Prior KM, Palmer TM, Young TP and Goheen JR (2016) Large herbivores promote habitat specialization and beta diversity of African savanna trees. *Ecology* **97**, 2640–2657.
- Raunonen P, Åkerblom M, Kaasalainen M, Casella E, Calders K and Murphy S (2015) Massive-scale tree modelling from TLS data. *ISPRS Annals of Photogrammetry, Remote Sensing & Spatial Information Sciences* **2**, 189–196.
- R Core Team (2018) *R: A Language and Environment for Statistical Computing*. Vienna: R Foundation for Statistical Computing. <https://www.R-project.org/>.
- Riginos C, Karande MA, Rubenstein DI and Palmer TM (2015) Disruption of a protective ant–plant mutualism by an invasive ant increases elephant damage to savanna trees. *Ecology* **96**, 654–661.
- Schepaschenko D, Chave J, Phillips OL, Lewis SL, Davies SJ, Réjou-Méchain M, Sist P, Scipal K, Perger C, Hérault B and Labrière N (2019) The Forest Observation System, building a global reference dataset for remote sensing of forest biomass. *Scientific Data* **6**, 1–11.
- Stanton ML, Palmer TM, Young TP, Evans A and Turner ML (1999) Sterilization and canopy modification of a swollen thorn acacia tree by a plant-ant. *Nature* **401**, 578–581.
- Ter-Mikaelian MT and Parker WC (2000) Estimating biomass of white spruce seedlings with vertical photo imagery. *New Forests* **20**, 145–162.
- Venables WN and Ripley BD (2002) *Modern Applied Statistics with S*. Fourth Edition. New York, NY: Springer.
- Whitham TG and Mopper S (1985) Chronic herbivory: impacts on architecture and sex expression of pinyon pine. *Science* **228**, 1089–1091.
- Yao W, Krzystek P and Heurich M (2012) Tree species classification and estimation of stem volume and DBH based on single tree extraction by exploiting airborne full-waveform LiDAR data. *Remote Sensing of Environment* **123**, 368–380.
- Young HE, Strand L and Altenberger R (1964) TB12: preliminary fresh and dry weight tables for seven tree species in Maine. *Maine Agricultural Experimental Station Technical Bulletin* **12**, 1–83.
- Young TP, Okello BD, Kinyua D and Palmer TM (1997a) KLEE: A long-term multi-species herbivore exclusion experiment in Laikipia, Kenya. *African Journal of Range & Forage Science* **14**, 94–102.
- Young TP, Stubblefield CH and Isbell LA (1997b) Ants on swollen-thorn acacias: species coexistence in a simple system. *Oecologia* **109**, 98–107.